IAC-04-A.P.12

NONLINEAR ATTITUDE CONTROL OF THE MICRO-SATELLITE ESEO

Morten Pedersen Topland and Jan Tommy Gravdahl

Department of Engineering Cybernetics
Norwegian University of Science and Technology
N-7491 TRONDHEIM
NORWAY

August 23, 2004

ABSTRACT

In this paper, attitude control of a spacecraft using thrusters and reaction wheels as actuators is studied. Linearization and Lyapunov theory is used to derive two linear and four nonlinear controllers. Three of the nonlinear controllers rely on cancellation of system nonlinearities, while the fourth is a sliding mode controller. By restricting the spacecraft inertia, simpler controllers can be found. Several controllers are compared in simulations. The simulations are based on data from the micro-satellite, European Student Earth Orbiter (ESEO).

1 INTRODUCTION

1.1 Background

The micro-satellite ESEO is part of the Student Space Exploration and Technology Initiative (SSETI), which is a project supported by the Education Office of the European Space Agency (ESA). Students from twelve different European countries participate in SSETI. More information on SSETI can be found in [1]. SSETI is also planning a satellite which will orbit the moon, the European Student Moon Orbiter (ESMO). Work on this satellite is about to begin, and the first student team to be recruited was the ESMO Attitude Determination and Control System (ADCS) team. This Norwegian team is based at the Norwegian University of Science and Technology (NTNU) in Trondheim and Narvik University College (HiN) in Narvik. The first task of the ESMO ADCS team was to do a case study of ESEO. The work presented in this article is part of this study, and its contents is based on [2].

1.2 Previous work

A standard reference on spacecraft dynamics is [3]. In [4] nonlinear attitude control of a spacecraft with thrusters and an arbitrary number of reaction wheels is studied, where the modified Rodrigues parameters are used to describe the attitude of the spacecraft. The use of Euler parameters or unit quaternions in attitude control problems, is studied by [5], but the results are applied to underwater vehicles. A nonlinear sliding mode controller is proposed by [6]. Vibration suppression during attitude control for flexible spacecraft is studied in [7], where various methods of transforming a continuous input torque to thruster torque pulses are presented.

At the Norwegian University of Science and Technology, [8], [9] and others have studied attitude control of satellites with magnetic coils and reaction wheels as actuators. Their results are part of the foundation of the NCUBE projects, where pico-satellites are launched into Earth orbit. For more information on NCUBE, see [10] and [11].

2 MODELING

2.1 Reference frames

To analyze the motion of a satellite, it is necessary to define reference frames, which this motion is relative to. These frames are the same as those used by [12] and [9].

The Earth Centered Inertial (ECI) frame is denoted $\mathcal{F}_i$, and has its origin at the center of the earth. Its unit vectors are x_i, y_i and z_i, where z_i is directed along the Earth's rotation axis. This frame is non-accelerated, that is inertial, which means that the laws of Newton apply.

The Earth Centered Earth Fixed (ECEF) frame is denoted $\mathcal{F}_e$, and has the same origin as $\mathcal{F}_i$. However $\mathcal{F}_e$ rotates relative to $\mathcal{F}_i$ with a constant angular velocity $\omega_e = 7.2921 \cdot 10^{-5}$ rad/s. This is the same as the an-

gular velocity of the Earth about its rotation axis. The unit vectors of $\mathcal{F}_e$ are x_e, y_e and z_e, where z_e is directed along the Earth's rotation axis.

The Orbit (O) frame, denoted $\mathcal{F}_o$, is located at the center of mass of the satellite, with the unit vectors x_o, y_o and z_o. z_o is pointing towards the center of the Earth, while x_o is pointing in the traveling direction of the satellite, tangent to the orbit. y_o is found using the right hand rule.

The Body (B) frame, denoted $\mathcal{F}_b$, has its origin at the center of mass of the satellite. This frame is fixed to the satellite body. Its unit vectors x_b, y_b and z_b are usually chosen to coincide with the spacecraft's principal axes of inertia. This simplifies the spacecraft's equations of motion. Rotations about x_b, y_b and z_b are called *roll*, *pitch* and *yaw* respectively.

2.2 Kinematics

This section is largely based on [3] and [13].

Definition 1 *A rotation matrix is a matrix $\mathbf{R} \in SO(3)$, defined by*

$$SO(3) = \left\{ \mathbf{R} | \mathbf{R} \in \mathbb{R}^{3 \times 3}, \mathbf{R}^T \mathbf{R} = \mathbf{1}, \det \mathbf{R} = \mathbf{1} \right\}, \quad (1)$$

where $\mathbf{1}$ is the identity matrix and $SO(3)$ is the special orthogonal group of order three. The rotation matrix transforms a coordinate vector from one reference frame to another, for instance the matrix $\mathbf{R}_o^b$ transforms $\mathbf{v}^o$ into $\mathbf{v}^b$: $\mathbf{v}^b = \mathbf{R}_o^b \mathbf{v}^o$.

The rotation matrix can be parameterized as

$$\mathbf{R}_{k,\theta} = \cos\theta \, \mathbf{1} + \mathbf{k}^\times \sin\theta + \mathbf{k}\mathbf{k}^T(1 - \cos\theta), \quad (2)$$

where $\mathbf{k}$ is an arbitrary unit vector in an arbitrary reference frame, and the angle θ represents the rotation about $\mathbf{k}$. The parameters $\mathbf{k}$ and θ are known as *angle-axis parameters*. Such a rotation is called a *simple rotation*. The elements of a rotation matrix $\mathbf{R}$ are called directional cosines, and can be arranged into column vectors:

$$\mathbf{R} = [\mathbf{c}_1, \mathbf{c}_2, \mathbf{c}_3] \quad (3)$$

In fact, these vectors are unit vectors, hence $\mathbf{c}_i^T \mathbf{c}_i = 1$. A composite rotation is represented by the product of two rotation matrices. The rotation from $\mathcal{F}_i$ to $\mathcal{F}_b$ can be expressed as $\mathbf{R}_i^b = \mathbf{R}_o^b \mathbf{R}_i^o$.

Definition 2 *The angular velocity vector of $\mathcal{F}_o$ relative to $\mathcal{F}_b$, written in $\mathcal{F}_b$, is denoted ω_{ob}^b, and is defined by the corresponding rotation matrix and its time derivative:*

$$\left(\omega_{bo}^b\right)^\times = \dot{\mathbf{R}}_o^b \left(\mathbf{R}_o^b\right)^T \quad (4a)$$

$$\omega_{bo}^b = -\omega_{ob}^b \quad (4b)$$

The cross product operator is defined by:

$$\omega^\times = \begin{bmatrix} 0 & -\omega_z & \omega_y \\ \omega_z & 0 & -\omega_x \\ -\omega_y & \omega_x & 0 \end{bmatrix}, \ \omega = \begin{bmatrix} \omega_x \\ \omega_y \\ \omega_z \end{bmatrix} \quad (5)$$

It can be shown that a similar relation exists for the directional cosines:

$$\dot{\mathbf{c}}_i = (\mathbf{c}_i)^\times \omega_{ob}^b \quad (6)$$

The Euler parameters, also called unit quaternions, give a representation of the rotation matrix without singularities. These parameters will be used in this paper.

Definition 3 *The Euler parameters are defined in terms of the angle-axis parameters, and are given by the scalar η and the vector ϵ. In coordinate form this is written*

$$\eta = \cos\frac{\theta}{2} \quad (7)$$

$$\epsilon = [\epsilon_1, \ \epsilon_2, \ \epsilon_3]^T = \mathbf{k} \sin\frac{\theta}{2} \quad (8)$$

where $\mathbf{k}$ is a unit vector. The Euler parameters satisfy the following property:

$$\eta^2 + \epsilon^T \epsilon = 1 \quad (9)$$

The rotation matrix $\mathbf{R}_{k,\theta}$ from (2) can now be expressed in Euler parameters as:

$$\mathbf{R}_{k,\theta} = \mathbf{R}_{\eta,\epsilon} = \mathbf{1} + 2\eta\epsilon^\times + 2\left(\epsilon^\times\right)^2 \quad (10)$$

As shown in [13], the kinematic differential equations in Euler parameters, written in $\mathcal{F}_b$ in reference to $\mathcal{F}_o$, are given as:

$$\dot{\eta} = -\frac{1}{2}\epsilon^T \omega_{ob}^b \quad (11a)$$

$$\dot{\epsilon} = \frac{1}{2}\left[\eta\mathbf{1} + \epsilon^\times\right]\omega_{ob}^b \quad (11b)$$

The actual attitude of a spacecraft is given by the rotation matrix $\mathbf{R} = \mathbf{R}_i^b$. Let $\mathcal{F}_o$ be a desired orientation, represented by $\mathbf{R}_d = \mathbf{R}_i^o$. This means that we want $\mathcal{F}_b$ to coincide with $\mathcal{F}_o$, that is $\mathbf{R} = \mathbf{R}_d$. In [5] the attitude error $\tilde{\mathbf{R}}$ is defined as

$$\tilde{\mathbf{R}} = \mathbf{R}_d^{-1}\mathbf{R} = \mathbf{R}_d^T \mathbf{R} \quad (12)$$

When the attitude error is zero, then $\tilde{\mathbf{R}} = \mathbf{1}$. When using unit quaternions, [5] has shown that the attitude error differential equations become

$$\dot{\tilde{\eta}} = -\frac{1}{2}\tilde{\epsilon}^T\tilde{\omega} \tag{13a}$$

$$\dot{\tilde{\epsilon}} = -\frac{1}{2}\left[\tilde{\eta}\mathbf{1} + \tilde{\epsilon}^\times\right]\tilde{\omega} \tag{13b}$$

where $\tilde{\omega}$ is the error in angular velocity. Note that (13) has the same form as (11). The error in angular velocity $\tilde{\omega}$ is given in reference to a desired reference frame $\mathcal{F}_d$. The error is zero when $\mathcal{F}_b$ and $\mathcal{F}_d$ have the same angular velocity. The angular velocity error is:

$$\tilde{\omega} = \omega_{db}^b = \omega_{ib}^b - \mathbf{R}_d^b\omega_{id}^d \tag{14}$$

This definition is used in [4] and [9].

2.3 Satellite dynamics

In this paper we will use the model of a rigid satellite with N reaction wheels as found in [4]. The dynamics can be written as

$$\dot{\mathbf{h}}^b = (\mathbf{h}^b)^\times \mathbf{J}^{-1}(\mathbf{h}^b - \mathbf{A}\mathbf{h}_a^b) + \tau_e \tag{15a}$$

$$\dot{\mathbf{h}}_a^b = \tau_a \tag{15b}$$

where $\mathbf{h}^b$ is the system angular momentum, which in $\mathcal{F}_b$ is given by

$$\mathbf{h}^b = \mathbf{I}\omega_{ib}^b + \mathbf{A}\mathbf{I}_s\omega_s, \tag{16}$$

and $\mathbf{h}_a^b$ is the N dimensional vector of axial angular momenta of the rotors:

$$\mathbf{h}_a^b = \mathbf{I}_s\mathbf{A}^T\omega_{ib}^b + \mathbf{I}_s\omega_s \tag{17}$$

The vector $\omega_s \in \mathbb{R}^N$ represents the axial angular velocities of the rotors relative to the body, while $\tau_e \in \mathbb{R}^3$ is the vector of external torques (e.g. thrusters and gravitation), $\tau_a \in \mathbb{R}^N$ is the vector of internal axial torques applied by the rigid body to the rotors, $\mathbf{A} \in \mathbb{R}^{3 \times N}$ is the matrix containing the axial vectors of the N rotors, and $\mathbf{I} \in \mathbb{R}^{3 \times 3}$ is the angular momentum, or inertia matrix, of the system, including the rotors. The matrix $\mathbf{I}_s = \text{diag}\{i_{s1}, \ldots, i_{sN}\} \in \mathbb{R}^{N \times N}$ is a diagonal matrix containing the axial moments of inertia of the rotors. The matrix $\mathbf{J} \in \mathbb{R}^{3 \times 3}$ is an inertia-like matrix defined as

$$\mathbf{J} = \mathbf{I} - \mathbf{A}\mathbf{I}_s\mathbf{A}^T \tag{18}$$

and can be interpreted as the inertia matrix of an equivalent system where all the rotors have zero axial moment of inertia. The angular velocity $\omega_{ib}^b \in \mathbb{R}^3$ of the body frame in reference to an inertial frame, can be written as

$$\omega_{ib}^b = \mathbf{J}^{-1}(\mathbf{h}^b - \mathbf{A}\mathbf{h}_a^b) \tag{19}$$

In this paper we will assume that the origin of $\mathcal{F}_b$ coincides with the origin of $\mathcal{F}_o$, and that $\mathcal{F}_b$ is oriented along the principal axes of inertia of the rigid body, which implies that the inertia matrix is diagonal, that is $\mathbf{I} = \text{diag}\{i_x, i_y, i_z\}$.

2.4 Error dynamics

A mathematical model of the error dynamics as a function of the error in angular velocity can be derived from equations (14) to (19). This results in the following model where the control objective is to make $\mathcal{F}_b$ coincide with $\mathcal{F}_o$:

$$\mathbf{h}^b = \mathbf{I}\left(\tilde{\omega} + \mathbf{R}_o^b\omega_{io}^o\right) + \mathbf{A}\mathbf{I}_s\omega_{\mathbf{s}} \tag{20a}$$

$$\mathbf{h}_a^b = \mathbf{I}_s\mathbf{A}^T\left(\tilde{\omega} + \mathbf{R}_o^b\omega_{io}^o\right) + \mathbf{I}_s\omega_s \tag{20b}$$

$$\dot{\mathbf{h}}^b = (\mathbf{h}^b)^\times\left(\tilde{\omega} + \mathbf{R}_o^b\omega_{io}^o\right) + \tau_e \tag{20c}$$

$$\dot{\mathbf{h}}_a^b = \tau_a \tag{20d}$$

$$\mathbf{J} = \mathbf{I} - \mathbf{A}\mathbf{I}_s\mathbf{A}^T \tag{20e}$$

We will assume a circular orbit where the angular velocity of $\mathcal{F}_o$ is given by $\omega_{io}^o = [0, -\omega_0, 0]$. It is shown in [2] that:

$$\begin{aligned}\mathbf{J}\dot{\tilde{\omega}} = &\ \omega_0\mathbf{J}(\mathbf{c}_2)^\times\tilde{\omega} - \tilde{\omega}^\times\mathbf{I}\tilde{\omega} + \omega_0\tilde{\omega}^\times\mathbf{I}\mathbf{c}_2 \\ &- \tilde{\omega}^\times\mathbf{A}\mathbf{I}_s\omega_s + \omega_0(\mathbf{c}_2)^\times\mathbf{I}\tilde{\omega} - \omega_0^2(\mathbf{c}_2)^\times\mathbf{I}\mathbf{c}_2 \\ &+ \omega_0(\mathbf{c}_2)^\times\mathbf{A}\mathbf{I}_s\omega_s + \tau_e - \mathbf{A}\tau_a\end{aligned} \tag{21}$$

2.5 Disturbance torques

There are several external disturbance torques affecting a spacecraft. In [3] the gravitational torque, the aerodynamic torque, radiation torques and the magnetic torque are studied. The aerodynamic torque is only applicable at low altitudes. In this paper, we will suppose that all disturbance torques can be neglected, except for the gravitational torque. Assuming circular orbit, [3] has shown that the gravity gradient written in the body frame $\mathcal{F}_b$ is

$$\tau_g = 3\omega_0^2(\mathbf{c}_3)^\times\mathbf{I}\mathbf{c}_3 \tag{22}$$

where $\mathbf{c}_3$ is defined in (3). The vector $\mathbf{c}_3$ transforms the z_b-axis to the z_o-axis. The constant ω_0 is defined by $\omega_0^2 = \mu/r_c^3$ where r_c is the orbit radius, $\mu = Gm_p = 3.986 \cdot 10^{14}Nm^2/kg$, G is the universal gravitational constant and m_p is the mass of the Earth.

2.6 Thruster modeling and control

ESEO will use one reaction wheel and thrusters for attitude control. The thrusters are on or off by nature. A reaction wheel on the other hand can give a continuous torque. This means that a continuous signal of commanded torques must be translated to pulses which decide

whether a thruster should be on or off. We will choose a bang-bang controller with dead-zone, presented in [7], where the thrusters are fired if the commanded torque is greater than a certain threshold value, as illustrated in figure 1. Tuning the size of the dead-zone, it is possible to emphasize fuel consumption by choosing it large, or place emphasis on accuracy by having a small dead-zone.
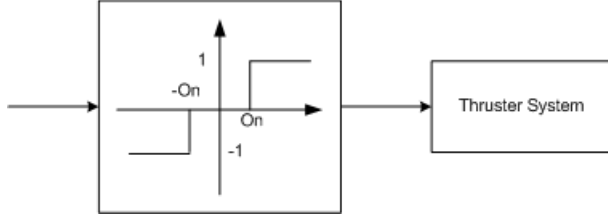

Figure 1: Bang-bang controller with dead-zone

3 CONTROLLER DESIGN

We will now derive controllers for ESEO, using Lyapunov's direct method and Krasovskii-LaSalle's theorem, which can be found in [14]. A linear controller based on a linearized system is presented first. We assume that the only external torques affecting the satellite are thruster torques τ_c and gravitational torques τ_g, thus $\tau_e = \tau_c + \tau_g$.

3.1 Local PD controller

The control law below is based on the linearized model of ESEO. If the parameters k_ϵ and k_ω satisfy

$$k_\epsilon >> i_s \tag{23a}$$
$$k_\omega > 0 \tag{23b}$$
$$k_\omega^2 > \omega_0^2 \left(i_z \left[2i_y - 2i_x - i_z \right] - \left[i_y - i_x \right]^2 \right) \tag{23c}$$

the control law

$$\tau_c = -k_\epsilon \mathbf{I} \tilde{\epsilon} - k_\omega \tilde{\omega} \tag{24a}$$
$$\tau_a = 0 \tag{24b}$$

makes the system (20) locally asymptotically stable. The details of the derivation is found in [2].

3.2 Global linear controller

We will now analyze how a linear controller can stabilize ESEO globally. To do this, we will use Lyapunov analysis.

Proposition 4 *The linear controller*

$$\tau_c = -k_0 \tilde{\epsilon} - \mathbf{C} \tilde{\omega} \tag{25a}$$
$$\tau_a = -\mathbf{E} \omega_s \tag{25b}$$

makes the equilibrium of (20) *globally asymptotically stable if* $i_y > i_x > i_z$, *where* $k_0 > 0$ *is a sufficiently large constant, and* $\mathbf{C} > 0$ *and* $\mathbf{E} > 0$ *are constant matrices. An obvious choice is* $\mathbf{C} = k_\omega \mathbf{1} > 0$ *and* $\mathbf{E} = k_s \mathbf{1} > 0$ *where* k_ω *and* k_s *are constants.*

Proof. We choose the following Lyapunov function candidate (LFC) V:

$$
\begin{aligned}
V &= \overbrace{\frac{1}{2} \left[\tilde{\omega}^T, \ \omega_s^T \right] \begin{bmatrix} \mathbf{I} & \mathbf{A} \mathbf{I}_s \\ \mathbf{I}_s \mathbf{A}^T & \mathbf{I}_s \end{bmatrix} \begin{bmatrix} \tilde{\omega} \\ \omega_s \end{bmatrix}}^{V_a} \\
&\quad - \frac{1}{2} \omega_0^2 \mathbf{c}_2^T \mathbf{I} \mathbf{c}_2 + k_0 \left(\tilde{\epsilon}^T \tilde{\epsilon} + [\tilde{\eta} - 1]^2 \right) \\
&\quad + \frac{3}{2} \omega_0^2 \mathbf{c}_3^T \mathbf{I} \mathbf{c}_3 + \frac{1}{2} \omega_0^2 \left(i_y - 3i_z \right) \\
&= \frac{1}{2} \tilde{\omega}^T \mathbf{I} \tilde{\omega} + \omega_s \mathbf{I}_s \mathbf{A}^T \tilde{\omega} + \frac{1}{2} \omega_s^T \mathbf{I}_s \omega_s \\
&\quad - \frac{1}{2} \omega_0^2 \mathbf{c}_2^T \mathbf{I} \mathbf{c}_2 + 2k_0 \left(1 - \tilde{\eta} \right) \\
&\quad + \frac{3}{2} \omega_0^2 \mathbf{c}_3^T \mathbf{I} \mathbf{c}_3 + \frac{1}{2} \omega_0^2 \left(i_y - 3i_z \right)
\end{aligned}
\tag{26, 27}
$$

The state vector is

$$\mathbf{x} = \left[\tilde{\omega}^T, \ \omega_s, \ \tilde{\eta}, \ \tilde{\epsilon}^T, \ c_{12}, \ c_{32}, \ c_{13}, \ c_{23} \right]^T$$

where c_{12}, c_{32}, c_{13} and c_{23} are the respective components of the vectors $\mathbf{c}_2$ and $\mathbf{c}_3$ defined in (3). The desired state vector is

$$\mathbf{x}^* = \left[0^3, \ 0^N, \ 1, \ 0^3, \ 0, \ 0, \ 0, \ 0 \right]^T .$$

The first three terms (V_a) and the fourth term in V represents the kinetic energy of the satellite, although it is not equal to its total kinetic energy. The fifth term comes from the attitude error where k_0 is a positive constant. The sixth term represents the potential energy of the satellite. The last term is constant in order to make V a true Lyapunov function, that is $V > 0$ and $V(\mathbf{x}^*) = 0$. In fact, V meets these requirements only when $i_y > i_x > i_z$, which is shown in [9]. It is shown in [2] that the time derivative of V_a is given by:

$$\dot{V}_a = \tilde{\omega}^T \tau_e + \omega_s^T \tau_a - \omega_0^2 \tilde{\omega}^T (\mathbf{c}_2)^\times \mathbf{I} \mathbf{c}_2 \tag{28}$$

The time derivative of V along the trajectories of (20) thus becomes:

$$
\begin{aligned}
\dot{V} &= \dot{V}_a - \frac{1}{2} \omega_0^2 \mathbf{c}_2^T \mathbf{I} \dot{\mathbf{c}}_2 - 2k_0 \dot{\tilde{\eta}} + \frac{3}{2} \omega_0^2 \mathbf{c}_3^T \mathbf{I} \dot{\mathbf{c}}_3 \tag{29} \\
&= \tilde{\omega}^T \tau_c + \omega_s^T \tau_a - \omega_0^2 \tilde{\omega}^T (\mathbf{c}_2)^\times \mathbf{I} \mathbf{c}_2 \\
&\quad + 3\omega_0^2 \tilde{\omega}^T (\mathbf{c}_3)^\times \mathbf{I} \mathbf{c}_3 - \omega_0^2 \mathbf{c}_2^T \mathbf{I} (\mathbf{c}_2)^\times \tilde{\omega} \tag{30} \\
&\quad + k_0 \tilde{\omega}^T \tilde{\epsilon} + 3\omega_0^2 \mathbf{c}_3^T \mathbf{I} (\mathbf{c}_3)^\times \tilde{\omega}
\end{aligned}
$$

Since all the terms are scalars, they can be freely transposed. Exploiting the fact that $(\tilde{\omega}^\times)^T = -\tilde{\omega}^\times$ we obtain:

$$\dot{V} = \tilde{\omega}^T \tau_c + \omega_s^T \tau_a + k_0 \tilde{\omega}^T \tilde{\epsilon} \qquad (31)$$

Combining (25) with (31), we get:

$$\dot{V} = -\tilde{\omega}^T \mathbf{C} \tilde{\omega} - \omega_s^T \mathbf{E} \omega_s \qquad (32)$$

Since $\mathbf{C} > 0$ and $\mathbf{E} > 0$, $\dot{V} \le 0$. Thus $\tilde{\omega} \to 0 \Rightarrow \dot{\tilde{\omega}} \to 0$ and $\omega_s \to 0 \Rightarrow \dot{\omega}_s \to 0$. Hence (21) becomes:

$$0 = -\omega_0^2 (\mathbf{c}_2)^\times \mathbf{I} \mathbf{c}_2 + 3\omega_0^2 (\mathbf{c}_3)^\times \mathbf{I} \mathbf{c}_3 - k_0 \tilde{\epsilon} \qquad (33)$$

The terms to the right are bounded because $\mathbf{c}_i$ is a unit vector and $\|\tilde{\epsilon}\| \le 1$. Hence there should be a large enough choice of k_0 which makes $\tilde{\epsilon} = 0$ the only solution, as proposed by [8]. In [2] it is shown that choosing $k_0 > 5.5432\,\omega_0^2 (i_y - i_z) \Rightarrow \tilde{\epsilon} \to 0$. Thus the equilibrium point will be globally asymptotically stable by Krasovskii-LaSalle's theorem. ∎

3.3 Lyapunov controller 1

In section 3.2 there were restrictions on the inertia matrix of the satellite. In case such restrictions are not met by a satellite, we will derive a nonlinear controller which does not have these restrictions.

Proposition 5 *The nonlinear controller*

$$\tau_c = -k_1 \tilde{\epsilon} - \mathbf{C} \tilde{\omega}$$
$$+ \omega_0^2 (\mathbf{c}_2)^\times \mathbf{I} \mathbf{c}_2 - 3\omega_0^2 (\mathbf{c}_3)^\times \mathbf{I} \mathbf{c}_3 \qquad (34a)$$
$$\tau_a = -\mathbf{E} \omega_s \qquad (34b)$$

makes the equilibrium of (20) *globally asymptotically stable, where* $\mathbf{C} > 0$ *and* $\mathbf{E} > 0$ *are constant matrices. A possible choice is* $\mathbf{C} = k_\omega \mathbf{1} > 0$ *and* $\mathbf{E} = k_s \mathbf{1} > 0$ *where* k_ω *and* k_s *are constants.*

Proof. Consider the following LFC:

$$V = V_a + 2k_1 (1 - \tilde{\eta}) \qquad (35)$$

where k_1 is a positive constant. The time derivative of V along the trajectories of (20) is given by:

$$\dot{V} = \tilde{\omega}^T \tau_c + \omega_s^T \tau_a - \omega_0^2 \tilde{\omega}^T (\mathbf{c}_2)^\times \mathbf{I} \mathbf{c}_2$$
$$+ 3\omega_0^2 \tilde{\omega}^T (\mathbf{c}_3)^\times \mathbf{I} \mathbf{c}_3 + k_1 \tilde{\omega}^T \tilde{\epsilon} \qquad (36)$$

Inserting (34) into (36), we get:

$$\dot{V} = -\tilde{\omega}^T \mathbf{C} \tilde{\omega} - \omega_s^T \mathbf{E} \omega_s \qquad (37)$$

Since $\mathbf{C} > 0$ and $\mathbf{E} > 0$, $\dot{V} \le 0$. Thus $\tilde{\omega} \to 0 \Rightarrow \dot{\tilde{\omega}} \to 0$ and $\omega_s \to 0 \Rightarrow \dot{\omega}_s \to 0$. Hence (21) becomes $k_0 \tilde{\epsilon} = 0 \Rightarrow \tilde{\epsilon} \to 0$. Thus the system is globally asymptotically stable according to the theorem of Krasovskii-LaSalle. ∎

3.4 Lyapunov controller 2

The preceding controllers do not use the reaction wheels directly as actuators for attitude control. It would be desirable to use the reaction wheels as actuators in the same way as the thrusters. This motivates an LFC where we omit ω_s from the state vector, and treat it as an external signal.

Proposition 6 *The nonlinear control laws*

$$\tau_c = -k_{\epsilon,1} \tilde{\epsilon} - \mathbf{C} \tilde{\omega} \qquad (38a)$$
$$\mathbf{A} \tau_a = k_{\epsilon,2} \tilde{\epsilon} + \mathbf{D} \tilde{\omega}$$
$$+ \omega_0 (\mathbf{c}_2)^\times \mathbf{A} \mathbf{I}_s \left(\mathbf{A}^T \tilde{\omega} + \omega_s \right) \qquad (38b)$$

make the equilibrium of the system (20) *globally asymptotically stable if* $i_y > i_x > i_z$, *where* $k_{\epsilon,1}$ *and* $k_{\epsilon,2}$ *are constants satisfying* $(k_{\epsilon,1} + k_{\epsilon,2}) > 0$, $(k_{\epsilon,1} + k_{\epsilon,2})$ *is sufficiently large, and* $\mathbf{C}$ *and* $\mathbf{D}$ *are constant matrices satisfying* $(\mathbf{C} + \mathbf{D}) > 0$. *Obvious choices which ensure this are* $\mathbf{C} = k_{\omega,1} \mathbf{1}$ *and* $\mathbf{D} = k_{\omega,2} \mathbf{1}$ *where* $k_{\omega,1}$ *and* $k_{\omega,2}$ *are constants and* $(k_{\omega,1} + k_{\omega,2}) > 0$.

Proof. Consider the LFC

$$V = \frac{1}{2} \tilde{\omega}^T \mathbf{J} \tilde{\omega} - \frac{1}{2} \omega_0^2 \mathbf{c}_2^T \mathbf{I} \mathbf{c}_2 + 2k_2 (1 - \tilde{\eta})$$
$$+ \frac{3}{2} \omega_0^2 \mathbf{c}_3^T \mathbf{I} \mathbf{c}_3 + \frac{1}{2} \omega_0^2 (i_y - 3i_z) \qquad (39)$$

where k_2 is a positive constant. The state vector is

$$\mathbf{x} = \left[\tilde{\omega}^T, \ \tilde{\eta}, \ \tilde{\epsilon}^T, \ c_{12}, \ c_{32}, \ c_{13}, \ c_{23} \right]^T,$$

and the desired state vector is

$$\mathbf{x}^* = \left[0^3, \ 1, \ 0^3 \ 0, \ 0, \ 0, \ 0 \right]^T.$$

The first and second term in V represent the kinetic energy of the satellite. The other terms are the same as in the LFC (26). This means that V is a Lyapunov function if $i_y > i_x > i_z$. To calculate $\dot{V}$, we will use (21):

$$\dot{V} = \tilde{\omega}^T \mathbf{J} \dot{\tilde{\omega}} - \frac{1}{2} \omega_0^2 \mathbf{c}_2^T \mathbf{I} \dot{\mathbf{c}}_2 - 2k_2 \dot{\tilde{\eta}} + \frac{3}{2} \omega_0^2 \mathbf{c}_3^T \mathbf{I} \dot{\mathbf{c}}_3 \qquad (40)$$

$$= \omega_0 \tilde{\omega}^T \mathbf{J} (\mathbf{c}_2)^\times \tilde{\omega} + \omega_0 \tilde{\omega}^T (\mathbf{c}_2)^\times \mathbf{I} \tilde{\omega}$$
$$- \omega_0^2 \tilde{\omega}^T (\mathbf{c}_2)^\times \mathbf{I} \mathbf{c}_2 + \omega_0 \tilde{\omega}^T (\mathbf{c}_2)^\times \mathbf{A} \mathbf{I}_s \omega_s$$
$$+ \tilde{\omega}^T \tau_g + \tilde{\omega}^T \tau_c - \tilde{\omega}^T \mathbf{A} \tau_a$$
$$- \omega_0^2 \mathbf{c}_2^T \mathbf{I} (\mathbf{c}_2)^\times \tilde{\omega} + k_2 \tilde{\omega}^T \tilde{\epsilon} + 3\omega_0^2 \mathbf{c}_3^T \mathbf{I} (\mathbf{c}_3)^\times \tilde{\omega} \qquad (41)$$

Note that several terms have disappeared since $\tilde{\omega}^T \tilde{\omega}^\times = 0$. Transposing some terms, we get:

$$\dot{V} = \omega_0 \tilde{\omega}^T (\mathbf{c}_2)^\times (\mathbf{I} \tilde{\omega} - \mathbf{J} \tilde{\omega} + \mathbf{A} \mathbf{I}_s \omega_s) + \tilde{\omega}^T \tau_c$$
$$- \tilde{\omega}^T \mathbf{A} \tau_a + k_2 \tilde{\omega}^T \tilde{\epsilon} \qquad (42)$$

$$= \omega_0 \tilde{\omega}^T (\mathbf{c}_2)^\times \mathbf{A} \mathbf{I}_s \left(\mathbf{A}^T \tilde{\omega} + \omega_s \right) + \tilde{\omega}^T \tau_c$$
$$- \tilde{\omega}^T \mathbf{A} \tau_a + k_2 \tilde{\omega}^T \tilde{\epsilon} \qquad (43)$$

Inserting (38) into (43), we obtain:

$$\dot{V} = (k_2 - k_{\epsilon,1} - k_{\epsilon,2}) \tilde{\omega}^T \tilde{\epsilon} - \tilde{\omega}^T (\mathbf{C} + \mathbf{D}) \tilde{\omega} \quad (44)$$

Note that the control law for τ_a in (38) cancels the nonlinearities in $\dot{V}$. This is only possible if the reaction wheels are able to give torques about all three axes of rotation. If this is not the case, the thrusters should be used. We will get the same result for $\dot{V}$, if we choose to cancel the nonlinearities with τ_c instead. Choosing $k_2 = k_{\epsilon,1} + k_{\epsilon,2}$, we get:

$$\dot{V} = -\tilde{\omega}^T (\mathbf{C} + \mathbf{D}) \tilde{\omega} \quad (45)$$

Since $(\mathbf{C} + \mathbf{D}) > 0$, $\dot{V} \leq 0$. Thus, we have proved that $\tilde{\omega} \to 0 \Rightarrow \dot{\tilde{\omega}} \to 0$. We will now apply Krasovskii-LaSalle's theorem. When $\dot{\tilde{\omega}} = \tilde{\omega} = 0$, (21) becomes:

$$0 = -\omega_0^2 (\mathbf{c}_2)^\times \mathbf{I} \mathbf{c}_2 + 3\omega_0^2 (\mathbf{c}_3)^\times \mathbf{I} \mathbf{c}_3 - k_2 \tilde{\epsilon} \quad (46)$$

The constant k_2 must be chosen large enough to make $\tilde{\epsilon} = 0$ the only possible solution to this equation. Since this is the same equation as (33), choosing $k_2 > 5.5432 \, \omega_0^2 \, (i_y - i_z)$ yields a globally asymptotically stable system according to Krasovskii-LaSalle's theorem. ∎

3.5 Lyapunov controller 3

In section 3.4 there are restrictions on the inertia matrix of the satellite. The next controller will not have such restrictions.

Proposition 7 *The nonlinear control laws*

$$\tau_c = -k_{\epsilon,1} \tilde{\epsilon} - \mathbf{C} \tilde{\omega} \quad (47a)$$

$$\mathbf{A} \tau_a = k_{\epsilon,2} \tilde{\epsilon} + \mathbf{D} \tilde{\omega} + \omega_0 (\mathbf{c}_2)^\times \mathbf{A} \mathbf{I}_s \left(\mathbf{A}^T \tilde{\omega} + \omega_s \right)$$
$$- \omega_0^2 (\mathbf{c}_2)^\times \mathbf{I} \mathbf{c}_2 + 3\omega_0^2 (\mathbf{c}_3)^\times \mathbf{I} \mathbf{c}_3 \quad (47b)$$

make the equilibrium of the system (20) *globally asymptotically stable, where $k_{\epsilon,1}$ and $k_{\epsilon,2}$ are constants satisfying $(k_{\epsilon,1} + k_{\epsilon,2}) > 0$, and $\mathbf{C}$ and $\mathbf{D}$ are constant matrices satisfying $(\mathbf{C} + \mathbf{D}) > 0$. Obvious choices which ensure this are $\mathbf{C} = k_{\omega,1} \mathbf{1}$ and $\mathbf{D} = k_{\omega,2} \mathbf{1}$ where $k_{\omega,1}$ and $k_{\omega,2}$ are constants and $(k_{\omega,1} + k_{\omega,2}) > 0$.*

Proof. We will consider the following LFC V where k_3 is a positive constant:

$$V = \frac{1}{2} \tilde{\omega}^T \mathbf{J} \tilde{\omega} + 2k_3 (1 - \tilde{\eta}) \quad (48a)$$

This LFC is almost the same as (39), but two terms are removed. $\dot{V}$ becomes:

$$\dot{V} = \tilde{\omega}^T \mathbf{J} \dot{\tilde{\omega}} - 2k_3 \dot{\tilde{\eta}} \quad (49)$$
$$= \omega_0 \tilde{\omega}^T \mathbf{J} (\mathbf{c}_2)^\times \tilde{\omega} + \omega_0 \tilde{\omega}^T (\mathbf{c}_2)^\times \mathbf{I} \tilde{\omega}$$
$$- \omega_0^2 \tilde{\omega}^T (\mathbf{c}_2)^\times \mathbf{I} \mathbf{c}_2 + \omega_0 \tilde{\omega}^T (\mathbf{c}_2)^\times \mathbf{A} \mathbf{I}_s \omega_s$$
$$+ 3\omega_0^2 \tilde{\omega}^T (\mathbf{c}_3)^\times \mathbf{I} \mathbf{c}_3 + \tilde{\omega}^T \tau_c \quad (50)$$
$$- \tilde{\omega}^T \mathbf{A} \tau_a + k_3 \tilde{\omega}^T \tilde{\epsilon}$$

Transposing the first term, and using the definition of $\mathbf{J}$ in (20), we obtain:

$$\dot{V} = \omega_0 \tilde{\omega}^T (\mathbf{c}_2)^\times \mathbf{A} \mathbf{I}_s \left(\mathbf{A}^T \tilde{\omega} + \omega_s \right)$$
$$- \omega_0^2 \tilde{\omega}^T (\mathbf{c}_2)^\times \mathbf{I} \mathbf{c}_2 + 3\omega_0^2 \tilde{\omega}^T (\mathbf{c}_3)^\times \mathbf{I} \mathbf{c}_3 \quad (51)$$
$$+ \tilde{\omega}^T \tau_c - \tilde{\omega}^T \mathbf{A} \tau_a + k_3 \tilde{\omega}^T \tilde{\epsilon}$$

Inserting (47) into (51), we get:

$$\dot{V} = (k_3 - k_{\epsilon,1} - k_{\epsilon,2}) \tilde{\omega}^T \tilde{\epsilon} - \tilde{\omega}^T (\mathbf{C} + \mathbf{D}) \tilde{\omega} \quad (52)$$

The control law for τ_a in (47) cancels the nonlinearities in $\dot{V}$. We choose $k_3 = k_{\epsilon,1} + k_{\epsilon,2}$, thus:

$$\dot{V} = -\tilde{\omega}^T (\mathbf{C} + \mathbf{D}) \tilde{\omega} \quad (53)$$

Since $(\mathbf{C} + \mathbf{D}) > 0$, $\dot{V} \leq 0$. Thus $\tilde{\omega} \to 0 \Rightarrow \dot{\tilde{\omega}} \to 0$, and the system is globally asymptotically stable according to the theorem of Krasovskii-LaSalle. ∎

3.6 Sliding mode controller

According to [14], sliding mode controllers are robust to system parameter uncertainties. Such uncertainties are often encountered in practice. A good example is change of a satellite's inertia when thruster fuel is consumed. We will define the error of a parameter α to be $\Delta \alpha = \alpha - \hat{\alpha}$ where the values denoted with a hat $(\hat{\cdot})$ are the best estimates, or nominal values, of the system parameters.

Proposition 8 *The sliding mode controller*

$$\tau_c = -\tau_{sgn} \quad (54a)$$

$$\mathbf{A} \tau_a = (\hat{\mathbf{h}}^b)^\times [\tilde{\omega} + \hat{\omega}_0 \mathbf{c}_2] + \frac{3}{2} \hat{\omega}_0^2 \mathbf{c}_3^T \hat{\mathbf{I}} \mathbf{c}_3$$
$$+ \hat{\omega}_0 \hat{\mathbf{J}} (\mathbf{c}_2)^\times \tilde{\omega} + \frac{1}{2} \hat{\mathbf{J}} \mathbf{P} \left[\tilde{\eta} \mathbf{1} + (\tilde{\epsilon})^\times \right] \tilde{\omega} \quad (54b)$$
$$+ \tau_{sgn,a}$$

$$\tau_{sgn} = \begin{bmatrix} \beta_x \text{sgn}(s_x) \\ \beta_y \text{sgn}(s_y) \\ \beta_z \text{sgn}(s_z) \end{bmatrix}, \ \tau_{sgn,a} = \begin{bmatrix} \beta_{a,x} \text{sgn}(s_x) \\ \beta_{a,y} \text{sgn}(s_y) \\ \beta_{a,z} \text{sgn}(s_z) \end{bmatrix} \quad (54c)$$

makes the equilibrium of the system (20) *globally asymptotically stable, where*

$$\beta_i + \beta_{a,i} \geq \delta_i + \beta_{0,i},$$

6

$\beta_{0,i} > 0$ *is a constant and the vector* $\delta = [\delta_x,\ \delta_y,\ \delta_z]^T$ *is given by:*

$$\delta = (\Delta \mathbf{h}^b)^\times \tilde{\omega} - (\Delta(\mathbf{h}^b \omega_0))^\times \mathbf{c}_2$$
$$+ \frac{3}{2}\mathbf{c}_3^T \Delta(\omega_0^2 \mathbf{I})\mathbf{c}_3 + \Delta(\omega_0 \mathbf{J})(\mathbf{c}_2)^\times \tilde{\omega} \qquad (55)$$
$$+ \frac{1}{2}\Delta \mathbf{J P}\left[\tilde{\eta}\mathbf{1} + (\tilde{\epsilon})^\times\right]\tilde{\omega}$$

The sign function $\operatorname{sgn}(\cdot)$ *is defined by:*

$$\operatorname{sgn}(s_i) = \begin{cases} 1, & s_i > 0 \\ 0, & s_i = 0 \\ -1, & s_i < 0 \end{cases} \qquad (56)$$

Proof. The first step in sliding mode control is to design a sliding manifold

$$\mathbf{s} = [s_x,\ s_y,\ s_z]^T,$$

and [15] suggest the following manifold where $\mathbf{s} = 0$ implies that $\tilde{\epsilon}$ and $\tilde{\omega}$ tend to zero. Define

$$\mathbf{s} = \tilde{\omega} + \mathbf{P}\tilde{\epsilon} \qquad (57)$$

where $\mathbf{P} > 0$. We must now design a control law for the system states to reach the sliding manifold. Consider the LFC

$$V = \mathbf{s}^T \mathbf{J s} \qquad (58)$$

Its time derivative along the trajectories of (20) is given as:

$$\dot{V} = \mathbf{s}^T \left(\mathbf{J}\dot{\tilde{\omega}} + \mathbf{J P}\dot{\tilde{\epsilon}}\right) \qquad (59)$$
$$= \mathbf{s}^T \left((\mathbf{h}^b)^\times [\tilde{\omega} - \omega_0 \mathbf{c}_2] + \frac{3}{2}\omega_0^2 \mathbf{c}_3^T \mathbf{I c}_3 \right.$$
$$+ \tau_c - \mathbf{A}\tau_a + \omega_0 \mathbf{J}(\mathbf{c}_2)^\times \tilde{\omega} \qquad (60)$$
$$\left. + \frac{1}{2}\mathbf{J P}\left[\tilde{\eta}\mathbf{1} + (\tilde{\epsilon})^\times\right]\tilde{\omega}\right)$$

Inserting (54) into (60), we get:

$$\dot{V} = \mathbf{s}^T \left((\Delta \mathbf{h}^b)^\times \tilde{\omega} - (\Delta(\mathbf{h}^b \omega_0))^\times \mathbf{c}_2 \right.$$
$$+ \frac{3}{2}\mathbf{c}_3^T \Delta(\omega_0^2 \mathbf{I})\mathbf{c}_3 + \Delta(\omega_0 \mathbf{J})(\mathbf{c}_2)^\times \tilde{\omega} \qquad (61)$$
$$\left. + \frac{1}{2}\Delta \mathbf{J P}\left[\tilde{\eta}\mathbf{1} + (\tilde{\epsilon})^\times\right]\tilde{\omega} - \tau_{sgn} - \tau_{sgn,a}\right)$$
$$= \mathbf{s}^T \left(\delta - \tau_{sgn} - \tau_{sgn,a}\right) \qquad (62)$$

Since $\beta_i + \beta_{a,i} \geq \delta_i + \beta_{0,i}$, we have:

$$\dot{V} \leq -\left(\beta_{0,x}|s_x| + \beta_{0,y}|s_y| + \beta_{0,z}|s_z|\right) \qquad (63)$$

For $\mathbf{s} \neq 0$, $\dot{V} < 0 \Rightarrow s \to 0$. Hence, we reach our manifold $\mathbf{s}$ in finite time, and the system is globally asymptotically stable. ∎

4 SIMULATION

4.1 Numerical values

The inertia matrix of ESEO is given by $\mathbf{I} = \operatorname{diag}\{4.3500,\ 4.3370,\ 3.6640\}$. ESEO has one reaction wheel about its y_b-axis, hence $\mathbf{A} = [0,\ 1,\ 0]^T$. The wheel inertia is given by $i_s = 4 \cdot 10^{-5}$ kgm^2, and the maximum angular velocity of the reaction wheel is given by $(\omega_s)_{max} = 5035$ rpm. Table 1 shows the nominal torques of the thrusters. The simulation altitude is 250 km above the surface of the Earth.

x_b-axis	0.0484 Nm
y_b-axis	0.0484 Nm
z_b-axis	0.0398 Nm

Table 1: Nominal thruster torques

4.2 Implementation of controllers

Since ESEO only has one reaction wheel, the cancellation of system nonlinearities cannot be done with the reaction wheel alone. Thus, the control laws are modified in order to let the thrusters cancel nonlinearities about the x_b and z_b-axis, while the reaction wheel takes care of the y_b-axis nonlinearities. Regarding the sliding mode controller, it is discussed in [14] that such controllers suffer from chattering. This problem can be solved by replacing the sign function with a saturation function, which leads to decreased accuracy:

$$\operatorname{sat}(s_i, \gamma) = \begin{cases} 1, & s_i > \gamma \\ 0, & |s_i| < \gamma \\ -1, & s_i < -\gamma \end{cases} \qquad (64)$$

In the implementation of the sliding mode controller, the saturation function is used instead of the sign function, and the gains β_i and $\beta_{a,i}$ are chosen constant, that is:

$$\beta_i + \beta_{a,i} = \beta_{0,i} > \delta_i$$

4.3 Simulations and results

A simple step simulation is performed, where the satellite has an initial spin. First with ideal conditions, that is no measurement noise and perfect estimates of system parameters (figure 2 to 5). Then with a 20 % uncertainty on the system inertial parameters, and finally with added white noise and perfect parameter estimates (figure 6 to 9). The second simulation results in approximately the same results as the first, so these plots are not included. The only difference is a slighlty slower rate of convergence to the desired attitude. The attitude is presented in Euler angles, where the three angles ϕ, θ and ψ give the rotation of a reference frame relative to another about the x, y and z-axis respectively. In the plots, these angles represent the rotation of $\mathcal{F}_b$ relative to $\mathcal{F}_o$. The desired

accuracy is $\pm 1°$. All Euler angles have the same desired value.

5 CONCLUSION

In this paper, a variety of nonlinear controllers are developed to control the attitude of a spacecraft using thrusters and reaction wheels as actuators. Note that simpler controllers are obtained if the diagonal inertia matrix of the spacecraft satisfies $i_y > i_x > i_z$. Simulations show that all controllers obtain a desired accuracy of $\pm 1°$ in Euler angles. Some of the controllers do not use the reaction wheel actively to control the satellite's attitude, but they perform just as well as the others. Whether or not the reaction wheel is used actively, the Euler angle θ converges faster than the other Euler angles and it has a higher degree of accuracy. This is due to the presence of the reaction wheel. Note that when using the reaction wheel actively to control the spacecraft's attitude, the reaction wheel reaches saturation quickly. It is observed that added noise to the measured states yields more thruster firings. This work will be part of a basis for the next SSETI project, ESMO.

6 ACKNOWLEDGMENTS

REFERENCES

[1] SSETI, P. R., "SSETI," [Online] Available from: URL http://sseti.gte.tuwien.ac.at/WSW4/, 2004, [Accessed 24 May 2004].

[2] Topland, M. P., *Nonlinear Attitude Control of the Micro-Satellite ESEO*, Master's thesis, Department of Engineering Cybernetics, Norwegian University of Science and Technology, Trondheim, Norway, 2004.

[3] Hughes, P. C., *Spacecraft Attitude Dynamics*, John Wiley & Sons, Inc., USA, 1986.

[4] Hall, C. D., Tsiotras, P., and Shen, H., "Tracking Rigid Body Motion Using Thrusters and Momentum Wheels," *Journal of the Astronautical Sciences*, Vol. 50, No. 3, 2002, pp. 311–323.

[5] Fjellstad, O. and Fossen, T. I., "Quaternion Feedback Regulation of Underwater Vehicles," *Proceedings of the Third IEEE Conference on Control Applications*, Glasgow, UK, 1994.

[6] Lee, J. G., Park, C. G., and Park, H. W., "Sliding-Mode Controller Design for Spacecraft Attitude Tracking Maneuvers," *IEEE Transactions on aerospace and electronic systems*, Vol. 29, No. 4, 1993, pp. 1328–1333.

[7] Song, G. and Agrawal, B. N., "Vibration suppression during attitude control," *Acta Astronautica*, Vol. 49, No. 2, 2001, pp. 73–83.

[8] Soglo, P. K., *3-aksestyring av gravitasjonsstabilisert satelitt ved bruk av magnetspoler*, Master's thesis, Department of Engineering Cybernetics, Norwegian University of Science and Technology, Trondheim, Norway, 1994.

[9] Kristiansen, R., *Attitude Control of a Microsatellite*, Master's thesis, Department of Engineering Cybernetics, Norwegian University of Science and Technology, Trondheim, Norway, 2000.

[10] Gravdahl, J., Eide, E., Skavhaug, A., Svartveit, K., Fauske, K., and Indergaard, F., "Three Axis Attitude Determination and Control System for a Picosatellite: Design and Implementation," *Proceedings of the 54th International Astronautical Congress*, Bremen, Germany, 2003.

[11] Riise, A.-R., Samuelsen, B., Sokolova, N., Cederblad, H., Fasseland, J., Nordin, C., Otterstad, J., Fauske, K., Eriksen, O., Indergaard, F., Svartveit, K., Furebotten, P., Sæther, E., and Eide, E., "Ncube: The First Norwegian Student Satellite," *Proceedings of The 17th AIAA/USU Conference on Small Satellites*, Logan, Utah, USA, 2003.

[12] Fossen, T. I., *Marine Control Systems*, Marine Cybernetics, Trondheim, Norway, 2002.

[13] Egeland, O. and Gravdahl, J. T., *Modeling and Simulation for Automatic Control*, Marine Cybernetics, Trondheim, Norway, 2001.

[14] Khalil, H. K., *Nonlinear Systems*, Pearson Education International Inc., Upper Saddle River, New Jersey, USA, 2000.

[15] Fu, L.-C., Tsai, C.-W., and Yeh, F.-K., "A Nonlinear Missile Guidance Controller with Pulse Type Input Devices," *Proceedings of the American Control Conference*, San Diego, California, USA, 1999.
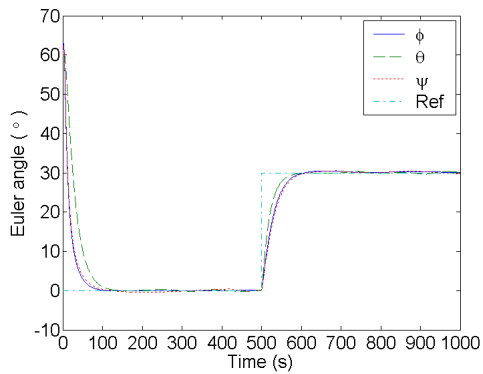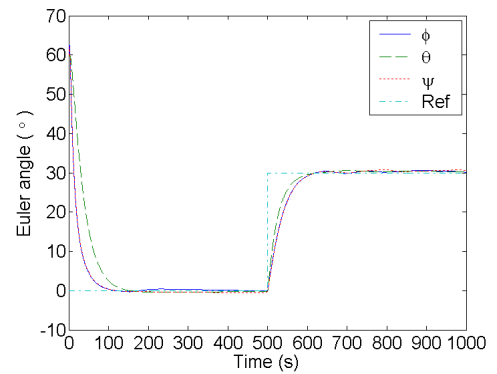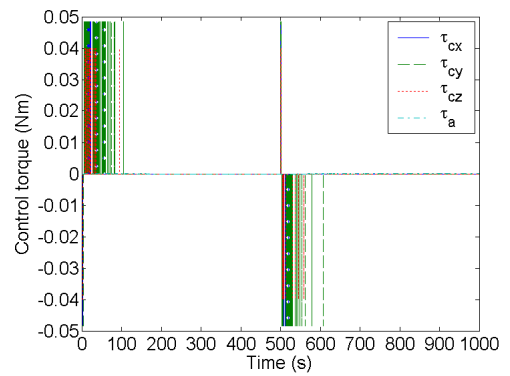
(a) Euler angles with reference
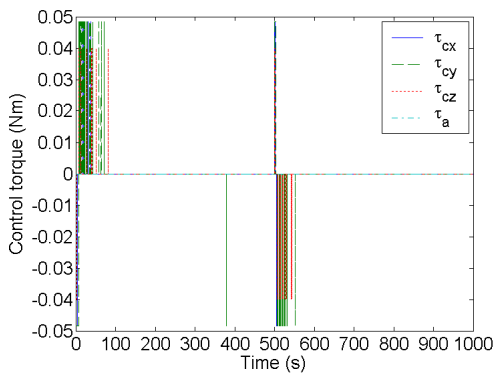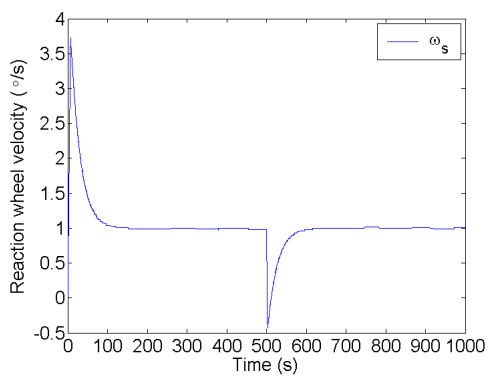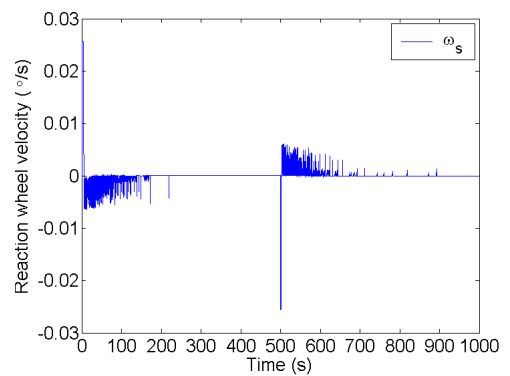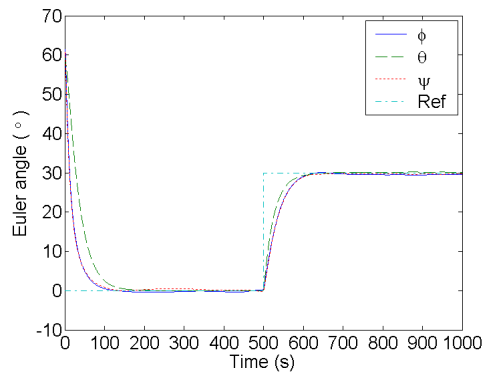

(b) Control torques

(c) Reaction wheel velocity

Figure 2: Simulation of local PD controller with ideal conditions

(a) Euler angles with reference

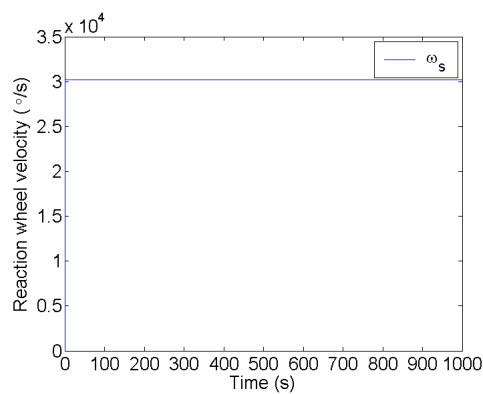(b) Control torques

(c) Reaction wheel velocity

Figure 3: Simulation of Lyapunov controller 1 with ideal conditions
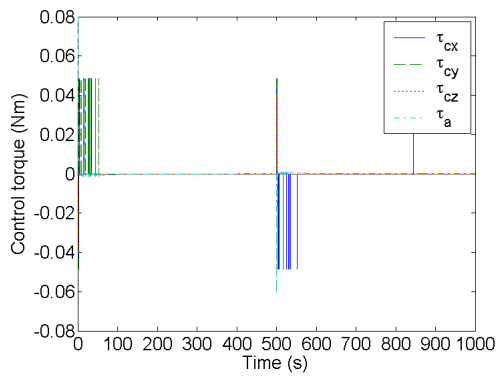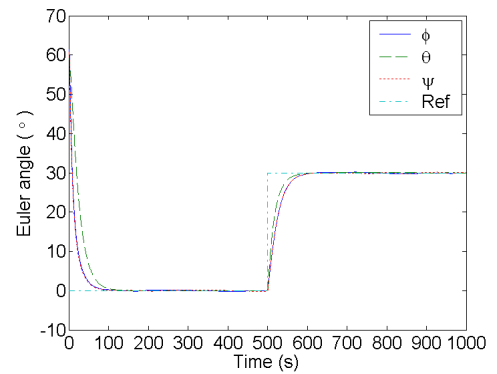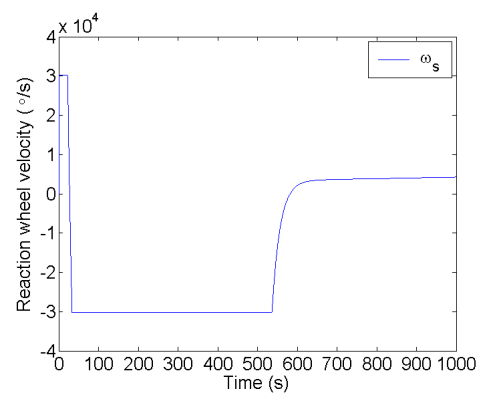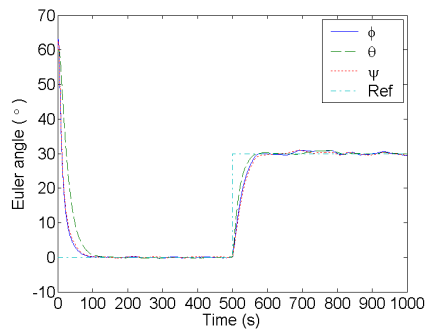
(a) Euler angles with reference
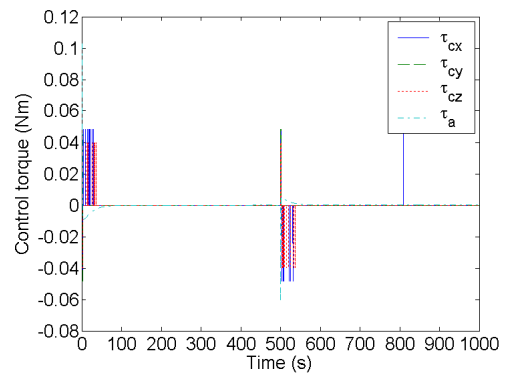
(b) Control torques

(c) Reaction wheel velocity

Figure 4: Simulation of Lyapunov controller 3 with ideal conditions

(a) Euler angles with reference

(b) Control torques

(c) Reaction wheel velocity

Figure 5: Simulation of sliding mode controller with ideal conditions

(a) Euler angles with reference
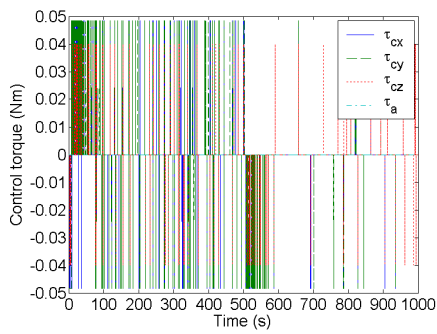
(b) Control torques

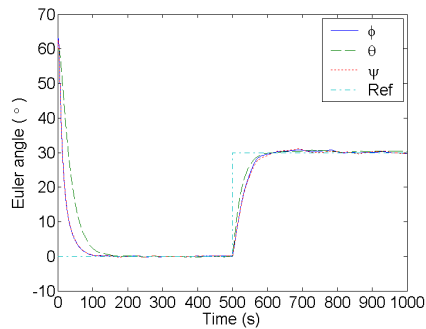Figure 6: Simulation of local PD controller with added white noise
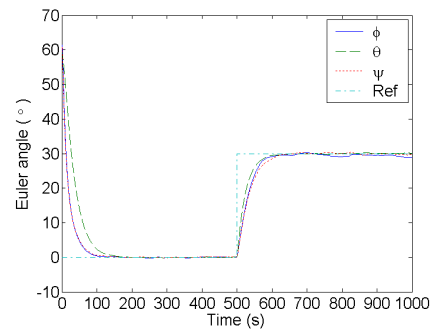
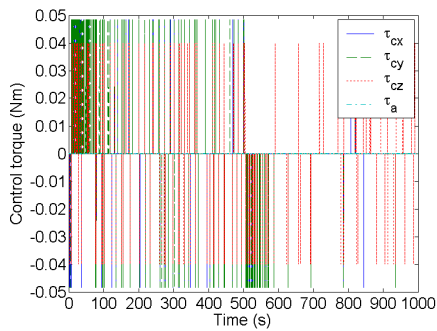
(a) Euler angles with reference
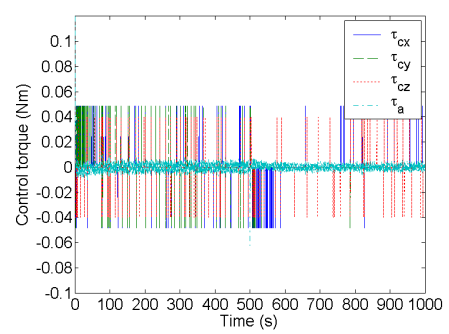
(b) Control torques

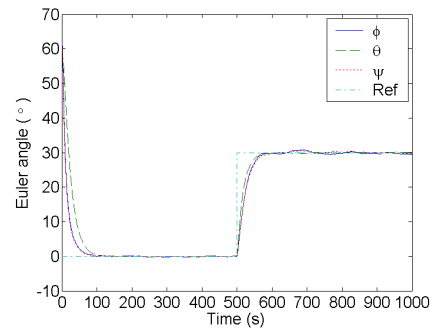Figure 8: Simulation of Lyapunov controller 3 with added white noise

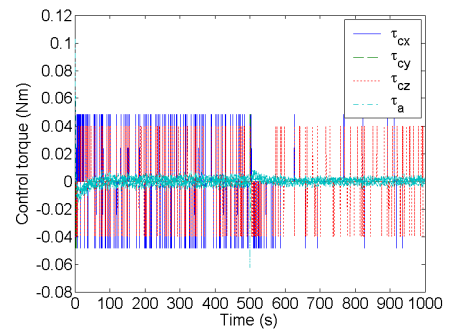(a) Euler angles with reference

(b) Control torques

Figure 7: Simulation of Lyapunov controller 1 with added white noise

(a) Euler angles with reference

(b) Control torques

Figure 9: Simulation of sliding mode controller with added white noise

11